THE LEVERAGE OF GRAY BALANCE IN CONTROLLING PERCEPTUAL AND QUANTITATIVE COLORIMETRY

Paul D. Fleming, Holly Jewell and Aniruddha D. Khandekar
Department of Paper Engineering, Chemical Engineering, and Imaging
Western Michigan University
Kalamazoo, Michigan

Abstract

The importance of monitoring and controlling the grayscale component of an image is demonstrated with two examples. One involves closed loop empirical color management, using a standard IT8.7/2 scanner target scanned and printed on a desktop ink jet printer. We show that a good color match can be obtained by working solely with the grayscale component of the image. The other example involves using a scanner profile to scan an IT8.7/2 target directly into CIELab. We show that the agreement between the measured original and the values in the scanned file is significantly improved by adjusting only the grayscale component of the target. These two examples, one without formal ICC color management and one with an ICC input profile for the scanner, show why controlling gray balance should be centermost in generating profiles for any device, input, display or output.

Introduction

The issues of managing and controlling color, from scanners to monitors to the digital printers/proofers and finally to printing presses, are serious ones for the printing and imaging industries. Accurate color control is vital in order to have predictable quality of final product, whether it be printed on substrate or displayed in an image editing program or a Web browser, and ultimately to satisfy customer expectations. The costs involved in controlling color for the designer/publisher/printer are both soft and hard. Soft costs include time spent by employees during prepress or pre publication, hard or soft proofing, film or plate output for printing presses, and on press. Hard costs include wasted ink and substrate used in makeready and time/money wasted on jobs that do not meet final customer specifications.

Great strides have been made in the printing industry in recent years toward applying scientific methods in the pressroom, as well as in the prepress area. Printing is becoming more and more science than art and every company, especially printing and media companies, must have a presence on the World Wide Web. This makes controlling agreement between displayed and printed color more important than ever. To accomplish this, standards have been established and Color Management methods have been developed. Essential to utilizing these methods are spectrophotometers and colorimeters, virtually unheard of by printers twenty years ago. These have now become necessary tools in all media industries (Bak 1997, Tolliver 1997, Adams 2000, Brues 2000 and Sharma 2003a).

To address the issues of accurate color control throughout the production process, color management (Adams 2000 and Brues 2000) systems have been developed. The International Color Consortium (ICC) was formed in 1993 by Adobe, Agfa, Apple, Kodak, Microsoft, Sun Microsystems and Silicon Graphics(Adams 2000, Brues 2000, Sharma 2003a, Green 1999e and ICC home page) to define the standards for color device characterization. This device characterization is presented in terms of specially formatted files, which have come to be called profiles. The current status of color management systems has been recently reviewed (Fleming 2002). The latest version (ICC 2001) of the ICC specification has been reviewed recently (McDowell 2002).

Unfortunately, the use of these color management systems has not yet solved all of the problems of color reproduction. One issue that has not received sufficient attention with these systems is that of gray balance, or color balance. The eye is very sensitive to a colorcast of an image, especially in highlights and neutral colors (Green 1999c) when viewed relative to "clean" white and black points. Thus, it is very important to faithfully reproduce the neutral and near neutral colors in an image. Therefore, any color management system and profile making algorithm should pay close attention to accurate reproduction of neutral and near neutral colors. In addition, as we shall see, gray balance has significant leverage in controlling the overall color of an image. Hence, in addition to eliminating problems with a colorcast, profile-making algorithms that enforce gray balance may converge more rapidly than ones that don't enforce it may.

Issues in Color Reproduction

In addition to becoming more scientific and technical, the printing and imaging industry is becoming more digital and more automated (Adams 1999).The advent of digital color and Color Management Systems (CMS) has moved the color management problem away from the pressroom and into the prepress and design areas.Customers are now designing images on their computers, but are (implicitly or explicitly) relying on the CMS support built into their image manipulation software (e.g.Adobe Photoshop,PageMaker,QuarkXPress,etc.) to make the necessary corrections so that what gets printed looks like what was created on the monitor.The latest versions of these programs fully support ICC color management, but anyone who has been through the transition between Photoshop 4,5.x, 6,7 and, now to, 8 (Sharma 2002c), knows it has been a "rocky road" to get there.

A large part of the problem of handling color lies in the inherent differences between the mechanisms by which different input, display and output devices perceive color (Williamson 1997, Samworth 1998, Rich 1997, Martens 1997 and Zhang 1997). Computer displays are generally based on the Additive Color Theory (Green 1999a,Pfiffner 1994 and Schildgen 1998a) and are represented in terms of differing amounts of Red, Green and Blue (RGB). On the other hand, printing ink on substrate is based on the Subtractive ColorTheory (Green 1999a,Pfiffner 1994 and Schildgen 1998b) that generally employs differing levels of Cyan,Magenta,Yellow and Black (CMYK).The problem is further complicated by the fact that the same RGB image looks different on different monitors, even ones that are nominally identical.The growing acceptance of Liquid Crystal Display (Widman 1998 (LCD) monitors, in addition to the standard Cathode Ray Tube (CRT) monitors, further complicates the situation. Likewise, the same CMYK value printed on different devices using different colorants and different substrates look different (Fleming 2002) . Furthermore, the two color models span different portions, or gamuts,of the visible color space (Zhang 1997,Green 1999a, Pfiffner 1994 and Schildgen 1998a,b). Some colors representable in the RGB space cannot be printed in CMYK space, and vice versa. In particular, highly saturated primary colors are readily displayed, but cause serious problems in printing. If this didn't complicate things enough, most scanners work in an RGB space that is almost certainly different from any monitor.Thus, all of the monitor and scanner RGB spaces are different from one another and all printing CMYK spaces are different from one another. Hence, RGB and CMYK are called device dependent color spaces.

Previous attempts at addressing these problems have met with various levels of success.The ICC has made a great deal of progress in defining devices and their profiles. However, we believe that profiling tools have not adequately addressed the issues of gray balance, or color balance, although these issues have been known for a long time (Archer 1954, Preucil 1964). Here we illustrate the power of gray balance and lightness in near neutrals in controlling the overall color of an image.There are also potential applications beyond just ink on substrate,such as in the medical field (Haneishi 1995), and the cosmetics industry (Imai 1997).

Objective

The objective of this research was to demonstrate the leverage that the gray balance (color balance and overall lightness) of an image,has on controlling its perceived color.We will illustrate this with two examples. One involves a "closed loop" (Adams 2000, Sharma 2003a and Fleming 2002) transformation from the scanner RGB color space to corrected (monitor) RGB color space, and from the corrected RGB color space to the CMYK color space of the output device.This part of the work was done without ICC profiles (it was done before we even had access to ICC profiles and profile making software), but it employed scanning an IT8.7/2 reflection target with an AGFA Arcus Plus scanner. We worked solely with the grayscale component of an image, using the "curves" feature of Photoshop. In iterative procedure was developed, which involved a statistical regression program along with measuring patches on a gray scale of the printed sample for each iteration.

The other example involves a different scanner (Heidelberg-LinoColor Saphir) and building an Input profile using Heidelberg Scanopen.The LinoColor software allows direct scanning into CIELab using a profile. We will show how the accuracy of the scan can be enhanced by adjusting the grayscale component of an IT8.7/2 reflection target scanned into CIELab.

Methodology

The tools used in this research were a Stouffer Gray Scale (Groff 1999b), a standard IT8.7/2 color reflection input target (ANSI 1993,Groof 1999a and Eastman Kodak),a spectrophotometer, a densitometer, two scanners, desktop computers (including both Apple Macintosh and Windows NT systems), an image editing program (Adobe Photoshop), and a desktop color printer.The color-input target chosen was the Kodak Q-60R1 (Eastman Kodak) color input target printed on Kodak Ektacolor paper. It was selected because it was designed to provide uniform mapping in the CIELAB color space, and is intended to be usable for both visual comparison and numerical analysis.

Example 1; Scanner and an Ink Jet Printer

The Epson Color Stylus 800 Printer was selected as the output device. It was selected because it is an ink jet printer that consistently delivers high ink densities and makes accurate measurements possible.The Color Stylus 800 is an example of a piezo drop on demand (DOD) ink jet printer (Nothman 1989a),as opposed to a thermal DOD ink jet printer (Nothman 1989b). Hewlett Packard DeskJet printers and Canon Bubble Jet printers are examples of thermal ink jet printers. The advantage of the piezo ink jet, which uses a pressure pulse to expel the ink droplets, is that it is less sensitive to temperature and humidity than a thermal ink jet, which uses a thermal pulse to create a vapor bubble in order to expel the ink droplets. The Color Stylus 800 is a high quality desktop printer capable of up to 1440 by 720-dpi resolution.

Standard Epson inks were used.These are known to be aqueous dye based inks. Epson printer drivers for Windows NT 4.0 were used to address the printer.All color adjustments available in the printer driver were disabled. It is generally believed that the printer driver addresses the printer as an RGB device.Thus,

Figure 1 Dot gain calibration image. The digital file for this image was provided by DICE America.

when a CMYK image is printed the printer driver converts it first to RGB and then back to the specific CMYK of the printer. Thus, we do not have full control of the inks output by the printer. A RIP (Raster Image Processor) or proprietary Epson code would be required for that. However, we have seen by image analysis (Lee 2002 and Fleming 2003) that 100% C prints Cyan ink only, 100% M prints Magenta ink only, etc. Thus, so long as the conversion mappings are smooth, the printer will behave as a CMYK device, although not necessarily as the same CMYK device as would appear if full control of the individual inks were available. In subsequent discussions references to CMYK "inks" refer to those of the apparent CMYK device, not the actual one. Nevertheless, our conclusions would not be altered if we had addressed the true device CMYK inks.

All images were output on the Color Stylus 800 at 720 dpi, with the tints treated using error diffusion dithering. Error diffusion dithering is a method of FM (Fischer 1989) or stochastic (Carli 1993 and Stanton 1994) screening, which is generally used for digital printers rather than conventional AM (Molla 1988 and Gustavson) digital halftone screening.

Four different substrates were considered for the ink jet printing portion of this project - Champion Ink Jet High Gloss, Weyerhaeuser Satin Ink Jet, Office Max Brite High Speed Xerographic Copy Paper, and Boise Cascade Copy Paper. After initial comparison testing, we selected the Weyerhaeuser Satin Ink Jet paper, because it has CIE (1931 and 1971) (Commission Internationale de l'Eclairage) L*a*b* values that are very similar to those of the Kodak Ektacolor paper.

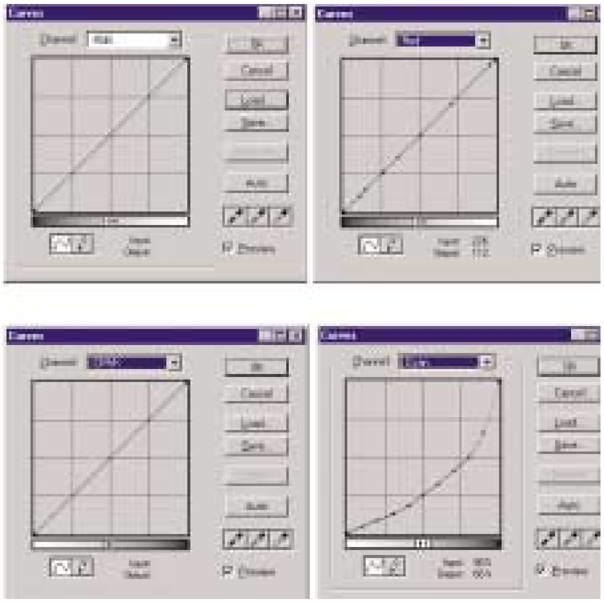

Figure 2. "Curves" windows for adjusting RGB and CMYK.

The first step in this segment of the research was the calibration of the printer to "zero dot gain". This process is often called linearization (Adams 2000), where an output device is adjusted to deliver a linear relationship between input and output. Such methods are also called "cut-back" curves, where halftone film dots are adjusted to match offset printing (Samworth 1998).

It involves outputting a calibration test image (this image was obtained from DICE America, see Figure 1), determining the ink percentage of each of the designated screen value areas, with a densitometer and the Murray-Davies (Murrey 1936) equation, and comparing the results with the specified values. The "Curves" feature of Adobe Photoshop was used to remap the measured tints to their posted values. A snapshot of the adjusted cyan curve is shown in Figure 2. Each of the four ink colors, (Cyan, Magenta, Yellow, and blacK), has its own separate curve, which was adjusted to reflect the unique values for that ink. By adjusting the input/output values for each ink, we are linearizing, or correcting for dot gain on the printer.

After generating the curves for each of the CMYK inks, they were applied to the test image and output to the printer. A comparison of the original and adjusted measured tints is given in Table 1. As seen there, the adjustments were effective in generating tint values within ±3% of the desired values.

The Kodak Q-60 target image (1997:04) was scanned on an AGFA Arcus Plus scanner along with a Stouffer Gray Scale. The separate Gray scale was included, even though the Q60 has an embedded gray scale, for three reasons. One is that the Stouffer Gray Scale has a brighter, "whiter" white than the Q60 ($L^*=96.0, a^*=-0.3, b^*=1.0$ versus $L^*=90.5, a^*=-1.6, b^*=7.4$ as measured with a Gretag SPM 60 Spectrophotometer in D65 mode with no filter). The second is that the Stouffer Scale is uniformly more neutral than the Q-60 (the average Chroma, $C^*=(a^{*2}+b^{*2})^{1/2}$, the smallness of which is a measure of how close the color is to neutral gray (Green 1999b), was measured to be 1.7 for the Stouffer and 2.0 for the Q-60). The third reason is that the physical size of the Stouffer scale makes it convenient to include with every scan, making it very convenient to adjust the color balance of a scan (especially if an IT8.7/2 and profiling software are unavailable).

The Q-60 and Gray Scale were scanned using the FotoLook 2.07.2 plug-in to Adobe Photoshop 4.0 at 600 dpi using the "set white/black points" option and no tone curve ($\gamma = 1$). The white and black points were chosen from the Stouffer scale. The image was scanned in as an RGB image and saved as an EPS file. In order to print, the file mode was changed to CMYK mode and output to the Color Stylus 800 using the Photoshop 4 default setting. This allows us to see how the Photoshop proprietary CMS, with default settings, handles the color space conversions from scanner to monitor to printer. This was the only CMS available at the time, since this work was originally done with Photoshop 4. The same effect can be obtained with Photoshop 6-8, by choosing Photoshop 4 default as the CMYK working space and assuming no distinction between scanner RGB and monitor RGB. Figure 3 shows that the resulting image was very dark and, because of the darkness, it was difficult to evaluate the overall color balance (as we'll see later it is quantitatively poor). One thing was clear - the printed image was very different from the original.

Figure 3 Image printed with default Photoshop CMS settings.

The Dmax patch on the Stouffer scale image showed values for the R, G and B in the 10 to 20 range. The values should have been closer to zero. This is an indication that the "set black point" function did not perform properly. Rather than rescan and try to "debug" the process, we "corrected" the image using the "Levels" function in Photoshop. The top snapshot in Figure 4

Device Linearization

Target Tint	10%	20%	30%	40%	50%	60%	70%	80%	90%	100%
Cyan Original	34	57	70	81	87	91	96	97	99	100
Cyan Adjusted	9	18	28	38	48	57	69	79	89	100
Magenta Original	27	49	66	77	86	90	94	96	99	100
Magenta Adjusted	11	19	28	38	47	59	67	79	89	100
Yellow Original	28	42	55	66	75	82	90	95	99	100
Yellow Adjusted	8	19	31	40	52	61	69	80	90	100
Black Original	21	39	56	68	79	84	88	92	96	100
Black Adjusted	11	18	28	38	49	58	69	81	91	100

Table 1. Device Linearization - Dot Values before and after linearization

shows that the black point of our image was cut off short of the full 256 shades of gray that should have been displayed. To correct this, the shadow indicator was moved to the right, as indicated in the bottom snapshot in Figure 4.

Because we scanned the Stouffer Gray Scale with the image, we were next able to move on to correct the color balance of the image by adjusting the gray balance. This was accomplished by following a process described below.

The steps for "Gray Balance Correction" are as follows:

1. Using the marquee tool, select a rectangular area that samples as much of one gray patch on the Stouffer Gray Scale image as can be selected without including the identifying number, or an adjacent box.

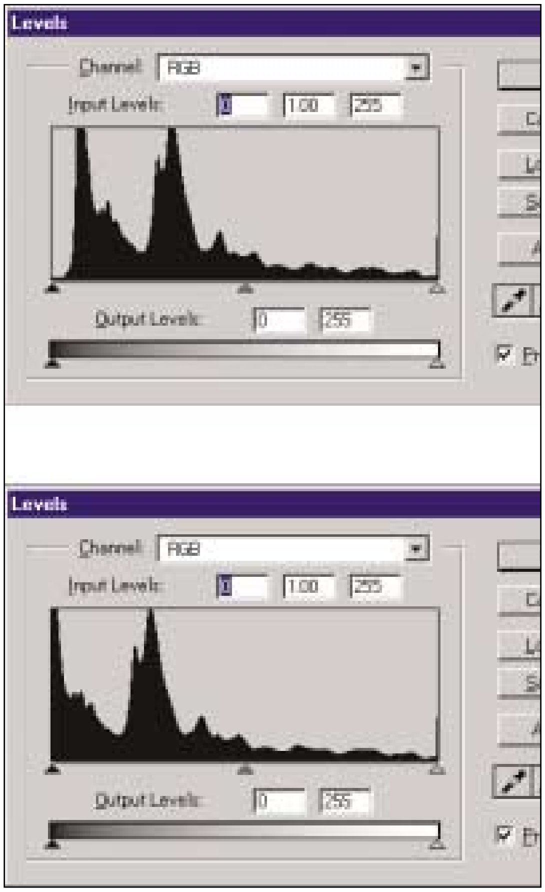

Levels

Channel: RGB

Input Levels: 0 1.00 255

Output Levels: 0 255

Levels

Channel: RGB

Input Levels: 0 1.00 255

Output Levels: 0 255

Figure 4 Original and adjusted "Levels".

2. Copy the selected area, open a "New" image area, and "Paste" the copied area into the new image screen.
3. Go to the Image menu, select "Image Size..." and change the image size to 1 pixel by 1 pixel. The resampling associated with this transformation generates the average of the RGB pixel values in the rectangular area. (The same average values could be obtained with the Image > Histogram menu pick. The advantage here is that the single pixel window can also preview the CMYK or Lab value in the Info Palette).

Figure 5. Image printed with zero dot gain correction curves, adjusted black point level, gray balance correction curves and custom ink settings.

4. Note the RGB values in the Info Palette window. To be a true neutral gray, all three values should be the same (Green 1999c). This is rarely true initially for any scanner. Generally, the values for the individual R, G and B components will all be different. Thus, it is necessary to make adjustments so that all three values are the same. This generally means changing two out of three values (usually adjusting to the value that falls in between.) For example, the average values may initially read: R-52, G-47, and B-50. In this case, the R and G should be adjusted to match the B.
5. Open the Curves. Select the Red, Blue, and Green channels one at a time. For each channel find the point on the curve that corresponds to the initial value that was shown on the Info Palette for that color, click on it and move it to the new adjusted value.
6. Save the new curves, click OK, and go to the next gray box, repeating all the steps.

Before we can assess the effects of adjusting the gray balance on the printed image, we must take into account the actual appearance of the printer's inks on the chosen substrate. Doing this eliminates the possibility that variation in the printed target image from the original is due to the specific color properties of the inks being different from the Photoshop 4 default. The Photoshop 4 default was called "SWOP" (2001) (Standards for Web Offset Publications) inks for "coated" paper. (Note that this differs from the "US Web Coated (SWOP) v2" ICC profile included with Photoshop 5-8, which are based on TR001(CGATS). The profile, now called Photoshop 4 Default CMYK, is, essentially, what was used to print Figure 3.) The account for ink and substrate was taken using the Custom Ink setup feature of Photoshop. To take advantage of this function, it is necessary to measure the chromaticity Yxy (CIE 1931) values of the printed Cyan, Magenta, Yellow, and blacK inks, as well as the values for the overprinted Red, Green, Blue, and 3-color Black, using a spectrophotometer or colorimeter.

The Yxy values were measured from the calibration image in Figure 1 using a Gretag SPM 60 spectrophotometer in D65 mode with no filter. This mode was chosen because it was the default mode for Photoshop 4 and earlier. These values were then entered into the Printing Inks Setup as Custom Inks, which is found under Color Settings. The Custom Ink is also adjusted to a Dot Gain of 0% in order to override the default 20% dot gain setting that Photoshop normally uses to simulate SWOP printing standards. This is to keep the resulting color separations consistent with the linearization calibration discussed above. From this, we saw that the black ink on the Satin paper was very neutral (L*=14.2, a*=.6 and b*=-.7).

The Monitor Setup was also given custom settings, to further standardize the transformation from the RGB to the CMYK color model. We chose to set the monitor to a $\gamma = 1$, and a white point of 6500°K and Trinitron phosphors. $\gamma = 1$ was set (regardless of the actual gamma of the monitor, which will vary from one monitor to the next) because that is what was assumed during the scanning process. The color temperature of 6500°K was chosen because that is consistent with using the spectrophotometer in D65 mode. (We did not have the means to construct a monitor profile at the time. Since we were working with scanner RGB in a closed loop with the printer, the monitor profile was in effect taken out of the loop. The choice of monitor parameters was made to provide a means to transform to the custom CMYK within the Photoshop 4 context.)

After applying the adjusted black point levels and the gray balance correction curves the file was converted from RGB to CMYK using the custom ink and monitor settings and medium GCR (Green 1999d (Gray Component Replacement). We then reprinted the target image, this time applying the linearized correction curves. The resulting printed image is shown in Figure 5. This looks much better than Figure 3. In order to quantify the improvement, the L*a*b* (41) values of the printed image were measured using the spectrophotometer, and these values are recorded in Table 2. The values from the original Stouffer scale and those from the uncorrected image in Figure 4 are included in Table 2 for comparison.

In order to quantify how far the printed gray value is from the Stouffer gray value, the values of

$$\Delta E = [(L_p^*-L_S^*)^2 + (a_p^*-a_S^*)^2 + (b_p^*-b_S^*)^2]^{1/2} \qquad (1),$$

are shown for each Stouffer gray level. The p subscript indicates measured printed value and the S subscript indicates measured Stouffer value.

The rms (root-mean-square) ΔE for Stouffer boxes 2-8 was reduced from 29.4 to 15.4, almost a factor of 2 reduction. The Stouffer number 1 box (white) and the Dmax (black) box were not included in the rms calculation since they depend primarily on the color of the paper and the black ink respectively. They don't vary with transformations that keep the black and white points fixed. The L*a*b* values that we expect for a balanced RGB gray should all have had values equal or near to zero (Samworth 1998), for both the a* and b"* components of the L*a*b* at every value of L*. This would indicate no color cast to the grays, and that they were "truly" gray. (Recall that in the L*a*b* system (CIE 1971), the L* represents the lightness or darkness of a color, the a* represents the opponent color values of red/green, and the b* represents the opponent color values of yellow/blue.) However, as is seen in Table 2, not only were the "L*" values different from those of the original Stouffer Gray Scale, but the a* and b* values show a definite color cast towards cyan. What this demonstrates is that even though the gray was balanced in scanner RGB, it did not print balanced. Thus, additional adjustments were necessary to print balanced gray values.

We note that the largest contribution to ΔE is from the difference in L* values. The image file can be adjusted to compensate for this by noting that the measured L* values from Figure 5 in Table 2, which were printed from known RGB values in the Stouffer Gray boxes, can be used to generate the transformation to the R=G=B values which will reproduce the measured L* values. This transformation is shown as a lookup table in Table 3. The values interpolated from this table to reproduce the measured values from the original are also shown in Table 3. This interpolation is then implemented using the "curves" function and the color picker window (see Figure 6).

After applying this new set of Curves, in addition to all the previously noted Curves, Levels, Custom Inks, GCR, and Monitor Settings, the target image was printed again. The resulting image is shown in Figure 7. The measured L*a*b* values of this printed image are given in

Table 2. Note that these L* values now are very close to those of the original Stouffer scale. The ΔE values are significantly reduced relative to those without the L* adjustment. The rms ΔE was reduced from 15.4 to 11.9, almost a 25% decrease. Note the corresponding rms ΔL value has been reduced from 11.5 to 0.5, essentially zero. The visual appearance is much better, but there is still a cyan cast evident in the negative values of both a and b. This is most noticeable when comparing to the original, because the Stouffer scale itself has a slight yellow cast. Note that the paper itself has a blue cast; so that the negative b values of the print from a gray-balanced image file result at least partially from the paper.

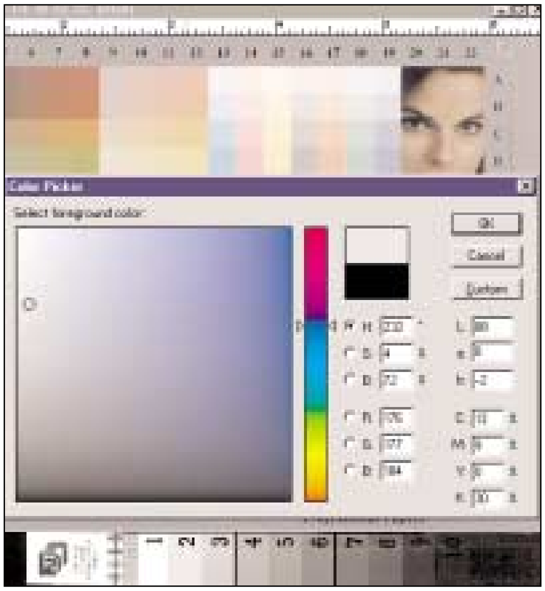

Figure 6 Color Picker Window.

Figure 7. Image reprinted with adjusted L values.

We can adjust the cyan cast of the print towards the yellow of the original by adjusting the RGB values to reflect the corresponding changes in a* and b*. We accomplish this by an iterative procedure. We start by changing the a* and b* values for the corresponding L* values by an amount equal to the difference between the original target value and the printed values. For example, for the #4 Stouffer Box, we adjust this box toward neutral. Thus, instead of adjusting R=G=B from 83 to 95 (R=G=B=95 corresponds to L*=67 and a*=b*=0) we adjust R=G=B from 83 to R=123, G=85 and G=77 (this corresponds to L*=67, a*=10 and b*=8). In principal, this should move the image 10 units of a* and 8 units of b* to achieve agreement with the original. This instead yielded a measured L*=60.0, a*=7.5 and b*=5.1. We see that this transformation over compensated. However, we can use these values along with the ones from Figures 5 and 7 to begin an iterative procedure to find the transformation that gets closest to the measured values.

In this iterative procedure, we regress the average file L*a*b* and RGB values for the box against the measured L*a*b* values, with a linear model, using the statistical program Minitab. Using the regression coefficients, we can estimate the file L*a*b* and RGB values which will reproduce the measured results. The transformation to these estimated values is performed and the resulting file printed with the custom inks and satin paper dot gain corrections applied. The resulting measured L*a*b* values are added to the database and the regressions are performed again to get new estimates. This procedure is continued until convergence is obtained. The final values were L*=70, a*=5, b*=6, R=120, G=98 and B=89. The measured values were L*=64.2, a*=-1.0 and b*=3.8 in good agreement with the original.

L*a*b values from Gretag SPM 60 in D65 mode with no filter.

Gray Scale Box #	1 (Paper)	2	3	4	5	6	7	8	Dmax
Original Stouffer									
L*	96.0	84.4	74.1	64.2	55.5	47.9	41.2	34.0	10.6
a*	-0.3	-0.1	-0.1	-0.1	-0.2	-0.3	-0.2	-0.4	0.8
b*	1.0	2.0	2.4	2.5	2.2	1.7	1.5	1.5	1.3
Uncorrected (Fig. 3)									
L*	94.1	72.5	53.0	36.3	16.9	14.7	14.7	14.8	14.9
a*	0.0	-16.5	-18.0	-16.0	-.72	0.3	0.3	0.3	0.3
b*	-3.1	-3.1	-4.9	-6.0	-1.6	-0.5	-0.6	-0.6	-0.5
ΔE	4.5	20.9	28.7	33.2	38.8	33.2	26.6	19.3	4.7
Satin before adjusted L* (Fig. 5)									
L*	95.0	84.5	73.3	59.1	49.3	39.1	20.5	15.1	14.9
a*	1.3	-3.1	-8.1	-9.7	-12.1	-11.9	-0.9	0.3	.3
b*	-3.4	-6.5	-4.9	-5.7	-4.4	-1.9	-5.4	-0.8	-.5
ΔE	4.8	8.9	10.8	13.6	15.0	15.0	21.9	19.1	4.7
Satin after adjusted L* (Fig. 7)									
L*	94.9	84.7	73.6	63.5	55.7	48.5	41.3	34.8	15.4
a*	1.3	-3.0	-8.1	-10.4	-11.0	-13.4	-8.7	-7.2	0.3
b*	-3.6	-6.6	-5.9	-5.7	-5.8	-3.2	-7.7	-7.7	-1.2
ΔE	5.0	9.1	11.5	13.2	13.4	14.0	12.4	11.5	5.4
Satin after adjusted a* & b* (Fig. 8)									
L*	95.1	84.2	73.6	64.2	55.7	47.5	40.8	34.3	15.1
a*	1.3	-0.4	-0.8	-1.0	1.0	0.9	0.6	-0.3	0.3
b*	-3.7	2.7	2.9	3.8	2.6	1.8	2.3	2.9	-0.7
ΔE	4.7	0.8	1.1	1.6	0.4	1.2	1.3	1.4	5.0

TABLE 2. L*a*b values from Gretag SPM 60 in D65 mode with no filter.

Gray Scale Box #s	#1 (Paper)	#2	#3	#4	#5	#6	#7	#8	Dmax
Printed L*	95.3	84.5	73.3	59.1	49.3	39.1	20.5	15.1	14.9
Average R=G=B	255.0	181.0	126.0	83.0	55.0	36.0	23.0	13.0	0.0
Desired L*	96.0	84.4	74.1	64.2	55.5	47.9	41.2	34.0	10.6
Interpolated R=G=B	255.0	181.0	126.0	95.0	71.0	53.0	39.0	32.0	0.0

Table 3. Lookup table - printed L* values for given average R=G=B values in file, and interpolated values for printing original Stouffer L* values.

Figure 8. Image reprinted with adjusted Lab values.

Applying this procedure to the #2 and #3 boxes and #5-#8 boxes as well, we generated a new set of curves, which were applied to the gray balanced image. Applying this corrected set of Curves to the image along with the other transformations, we printed again. This image is shown in Figure 8. The measured L*a*b* values of this last printout, shown in Table 2, differed by no more than 1.3 from the values of the original for L*, a* or b*. Furthermore the rms ΔE value has been further reduced to 1.2. This averages to a variation of less than 1 unit per direction in L*a*b* space, which is within the normal print to print variation and the degree of control from Photoshop (a variation of exactly 1 in each of L*, a* and b* would yield $\Delta E=\sqrt{3}=1.732$). In addition, the visual appearance is very close to the original Q-60R1 target, including good flesh tones, which are often hard to reproduce.

To verify this quantitatively, we compare some selected boxes from the Q60-R1 target. Based on the description of the standard (Adams 2000, ANSI, Groff 1990a and Eastman Kodak), we chose to measure A12, B12, C12, D12, E12, F12, G12, H12, I12, J12, K12, L12-L15 and L17-L19. These were chosen to sample many hues on the color wheel and at relatively high saturation or Chroma. These are typically the most difficult to reproduce using CMYK and the farthest from the grayscale from which the transformations were determined. The measured values from the prints compared with those from the original are shown in Table 4.

As seen in the Table, the ΔE values were very large for the initial print and are for the most part reduced significantly with each stage in our process. The rms ΔE value was reduced from 35.8 for Figure 3, to 20.0 for Figure 5, to 15.7 for Figure 7 and finally to 11.5 for Figure 8, when all measured boxes are considered (7 from the Stouffer and 18 from the Q-60R1). When only the 18 Q-60 boxes are considered, the values were 38.0, 21.5, 16.9 and 13.5, respectively. We note from the table that these high values are really dominated by the six most saturated boxes L13-L15 and L17-L19. These contribute rms ΔE values of 52.8, 33.4, 25.7 and 21.7 respectively. The original colors for these boxes are most certainly out of the printer's gamut. In fact, if the accurate profile from example 2, below, is used with the output profile for the Custom Ink Set Up, the calculated RMS ΔE for these 6 boxes is about 26, worse than from Figure 8. When these are not included (i.e. considering only A12-L12), the corresponding RMS ΔE values are 27.7, 11.5, 10.0 and 6.3. This latter value is satisfying since it amounts to a an average variation of only 3.6 units in each direction, approximately 3.6 % of the range of variation of the Q60-R1 target, all from optimizing to a tight fit to the Stouffer gray boxes.

Table 4. CIELAB coordinates from IT8.7/2 Target

Label	A12	B12	C12	D12	E12	F12	G12	H12	I12	J12	K12	L12	L13	L14	L15	L17	L18	L19
Original																		
L*	69.1	68.8	74.0	79.7	69.4	68.9	69.1	68.8	68.0	68.5	69.1	68.9	44.8	38.5	71.8	32.8	32.7	13.5
a*	22.5	20.5	12.2	-4.7	-20.2	-23.3	-23.0	-16.4	1.6	9.9	23.6	24.3	-32.9	62.9	14.2	52.0	-46.9	30.1
b*	7.1	18.8	34.4	42.3	28.2	8.4	-2.4	-16.4	-16.7	-17.2	-15.4	-3.3	-30.6	-26.9	90.4	39.4	30.4	-48.1
Figure 3																		
L*	51.2	51.6	59.1	66.6	55.7	54.9	55.4	54.6	50.3	49.7	48.2	48.8	24.9	29.3	55.4	27.1	14.8	15.3
a*	33.3	32.1	23.7	-16.9	-48.3	-49.8	-46.8	-20.1	3.5	10.8	23.7	33.7	11.2	32.7	22.5	8.1	0.4	0.3
b*	-3.7	8.1	26.6	43.0	34.1	18.2	3.8	-33.1	-43.2	-43.8	-41.9	-23.0	-30.4	-37.6	40.5	-3.8	-0.9	-1.4
ΔE	23.5	23.3	20.4	17.9	31.9	31.5	28.0	22.2	31.9	32.6	33.7	29.7	48.3	33.3	53.2	61.9	59.5	55.4
Figure 5																		
L*	70.6	71.3	75.6	81.0	69.0	68.8	69.7	73.6	67.5	66.9	65.5	68.9	48.1	41.6	73.8	37.5	21.9	24.6
a*	21.4	17.3	6.8	-14.2	-36.6	-35.6	-30.6	-20.2	0.9	8.3	21.6	25.7	-3.3	47.6	2.8	39.7	-4.9	11.7
b*	0.7	15.1	34.0	43.8	31.0	-7.8	-10.7	-28.1	-31.3	-30.4	-28.6	-11.8	-47.1	-29.4	62.6	14.1	0.2	-30.2
ΔE	6.7	5.5	5.7	9.6	16.6	12.3	11.2	13.2	14.6	13.4	13.8	8.7	34.1	15.8	30.1	28.6	52.9	27.9
Figure 7																		
L*	71.5	72.0	75.1	80.7	70.5	70.6	70.6	72.9	68.5	68.3	67.4	69.8	56.0	45.9	74.1	42.4	46.9	29.2
a*	19.4	16.5	10.8	-12.2	-30.4	-27.7	-24.9	-13.9	1.4	7.8	19.0	21.4	-17.9	41.9	4.1	35.9	-42.7	18.4
b*	-0.7	10.2	24.6	37.9	24.8	3.4	-8.9	-28.1	-28.9	-28.7	-26.4	-9.0	-40.8	-28.9	54.2	15.6	23.0	-44.7
ΔE	8.7	10.0	10.0	8.7	10.8	6.9	6.9	12.6	12.2	11.7	12.0	6.5	21.3	22.3	37.6	30.3	16.5	19.9
Figure 8																		
L*	73.3	73.6	75.5	81.0	69.5	70.7	71.5	71.7	70.0	69.3	70.5	71.8	54.9	50.5	75.4	46.5	46.9	28.2
a*	20.8	18.5	14.1	-6.0	-17.0	-16.7	-15.4	-6.7	9.7	14.6	24.7	22.4	-16.5	55.6	7.7	46.8	-41.1	19.1
b*	7.7	16.5	29.0	41.0	28.2	9.1	-2.2	-19.1	-21.2	-21.5	-15.9	-1.7	-38.6	-14.4	58.9	27.9	25.6	-42.4
ΔE	4.7	5.7	5.9	2.3	3.2	6.9	8.2	10.5	9.5	6.4	1.9	3.9	20.9	18.8	32.4	18.7	16.1	19.2

Table 4. CIELAB coordinates from A12, B12, C12, D12, E12, F12, G12, H12, I12, J12, K12, L12-L15 and L17-L19 boxes on IT8.7/2 Target

The values for the most saturated boxes are unsatisfying, but they are out of gamut anyhow. Nevertheless, they were still systematically reduced with each improvement in the match to the gray scale. This is achieved despite the fact the rms C* value for these 6 points is 65.4. Thus, these points are very far from the gray scale values (C*=0) and therefore present a severe test of the methods employed for this example, which cannot compensate for color gamut. The RMS C* value for the A12-L12 boxes is 28.0. The agreement with these relatively saturated boxes is truly remarkable.

While color can be controlled and manipulated colorimetrically, the final evaluation still comes down to "how it looks". A visual comparison of the final printed gray-balance adjusted image to the original Kodak Q-60R1 target reveals that it is, admittedly, not a perfect match. Indeed, the colorimetry data confirm this. However, it is a much closer match relative to the first print attempt.

This is as far as we can go with this example. Our method of closed loop color matching is both time-consuming and tedious. It would not be used in practice. Instead, one would build accurate (Sharma 2003a, Fleming 2002, Sharma 2002, 2003b, 2003c) ICC profiles for the scanner and printer and be done with it. What would be missed in this, now easy process with today's ICC profiling tools, is where the leverage is and how to get to the "best" final profile. The message to profile software developers is to pay attention to gray balance and, if necessary, give a higher weight to values fit near to a neutral gray (C*=0). After all this is consistent with the human visual experience, where the human eye is very sensitive to deviations from a neutral gray (Green 199c), especially when a good white point and black are available. This leverage of gray balance in color transformations is illustrated further with the next example, in this case using an ICC scanner profile.

Example 2; Scanner with an ICC profile

This case involves building an ICC profile for the scanner and using the generated profile to for "calibration" of the scan. The scanner used in this case is a LinoColor Saphir scanner and the scanning software was Heidelberg LinoColor Elite 6.0. The Calibration setting in LinoColor Elite accepts an ICC profile in the Calibration setting of the scan dialog box.

A profile was generated using Heidelberg Scanopen 4.05, which has been shown (Sharma 2003a, Fleming 2002, Sharma 2002, 2003b, 2003c) to yield accurate profiles. To accomplish this, a

DE values for original and grayscale corrected scan

	Average ΔE	RMS ΔE	Average Grayscale ΔE	RMS Grayscale ΔE	Average Saturated ΔE	RMS Saturated ΔE
Raw Scan	5.60	5.91	6.10	6.39	6.31	6.39
Corrected Scan	2.43	2.94	1.53	2.22	2.28	2.56

Table 5. DE values for original and gray scale corrected scan for the LinoColor Saphir scanner

different Kodak Q60 (1997:8) target was scanned on the Saphir scanner using LinoColor Elite, with scanner RGB as the Calibration setting and the scanned image was saved as an uncompressed RGB Tiff file. The Lab and XYZ values were measured (Rong 2002), using a GretagMacbeth Spectroscan T and MeasureTool in D50 mode, and entered into the standard text file format. The actual measurements for the target were used to adjust for differences between the actual print that we had and the batch average. For example the Blue patch, I19, was measured to be L*=34.1, a*=8.9, b*=-41.2 versus L*=33.8, a*=13.9, b*=-45.1 for the batch average. This corresponds to a ΔE=6.4 between the two values. The average ΔE, between measured and batch patches, was 3.5 and the RMS ΔE was 3.7. Scanopen was used with the image file and the data file to generate the input profile for the Saphir scanner.

The Q60 target was then rescanned using LinoColor Elite with the new profile used as the "Calibration". The image was saved as an uncompressed Lab Tiff file. The average Lab values for each Q60 patch were then read using our own program(Sharma 2003a, Fleming 2002, Sharma 2002, 2003b, 2003c). These values were entered into Microsoft Excel along with those from the measurement file. The overall average and RMS ΔE values were calculated along with the values for some subsets. The results are summarized in Table 5. The grayscale values were obtained from the 24 patches on the bottom of the target and A16-L16, which are also near neutral. The saturated values were combined from A13-L13 (Cyan), A14-L14 (Magenta), A15-L15 (Yellow), A17-L17 (Red), A18-L18 (Green) and A19-L19 (Blue). The values from the scan are fair, but not as good as obtained with other scanners(Sharma 2003a, Fleming 2002, Sharma 2002, 2003b, 2003c).

In order to improve the fit of the values, the Lab values for selected grayscale patches were adjusted to be close to the measured values, using a procedure similar to that described above. To facilitate this, a custom RGB working space profile (called IdealD50) was constructed. In this working space, R, G and B are proportional to the X, Y and Z tristimulus values, respectively. The point of this working space is that there is no "gamut clip" associated with transforming from Lab to RGB and back again. Thus, the scanned Lab file was transformed to the RGB, with this special profile and the RGB values for selected grayscale patches were adjusted to yield the measured Lab values using the Color Picker in Photoshop. Only the patches along the bottom of the chart were used for this adjustment, but similar results should be obtainable using A16-L16. The image was converted back to Lab and saved as a new Tiff file. The new average patch values were determined using our program and the results are summarized in Table 5.

The results for grayscale corrected image show that the grayscale ΔE values are reduced significantly from the original scan, as expected, but the saturated colors are reduced almost as much. The overall ΔE values have been more than cut in half and are comparable to other

results(Sharma 2003a, Fleming 2002, Sharma 2002, 2003b, 2003c), merely by adjusting along the grayscale line of the target. Once again, we see the significant leverage that gray balance has on reproduction of the image.

To apply this result to scans of other images on this scanner, one would scan the original into Lab, using the profile. The file would be converted into IdealD50 RGB by setting that profile as the working space (or alternatively performing a convert to profile on the scanned image, using IdealD50). The saved curves' file would then be loaded and applied. The resulting image can then be converted to Lab or to any desired RGB or CMYK working spaces. This was, in fact, done in preparation for printing on a color laser printer and a Flexographic press (Khandekar 2001 and in preparation). A new profile could be constructed from the original and the resulting transformation, using methods developed by Sharma (200b), et. al. The resulting profile would then be treated like any other input profile.

Conclusion

We have shown two examples where the gray balance of an image has so much leverage that the whole image can be brought into colorimetric agreement with the original by adjusting only the near gray portion of the image. This observation can be used to adjust a scanned image, even when ICC profiling tools are unavailable. In at least one case, the accuracy of generic scanner profile can be improved by almost an order of magnitude, by adjusting the gray balance (Rong 2002 and 2003).

Application of Results

These results can be used to improve the convergence algorithms used by profiling software. Optimization paths based on accuracy along the gray (C*=0) line of Lab space should lead to rapid convergence and the resulting profile should be visually satisfying because of the human sensitivity to gray balance. Even algorithms based on advanced mathematical techniques (Ker 1997) can be enhanced using these results.

The results of this research are applicable throughout the printing and imaging industries. There are also potential applications beyond just ink on substrate, such as in the medical field (Haneishi 1997), and the cosmetics industry (Imai 1997). The results we have presented can be applied to any substrate/ink/scanner/printer combinations, (including lithography, flexography, gravure, and various nonimpact printing methods). Therefore, there is much potential for further research in this area.

Recently, Bala (2001) has questioned whether C*=0 is the appropriate human perceived criterion for a true neutral gray. He suggested, based on a panel of observers, that the preferred gray was shifted toward negative a* and b*. His results, however, do not change our conclusions, because his "shifted gray point" would still be considered near neutral to the same extent that the Stouffer patches and the grayscale patches on the IT8 charts are near neutral.

REFERENCES

Adams, R. M. and F. J. Romano, 1999. Computer to Plate: Automating the Printing Industry, GATFPress, Second Edition.

Adams, R. M. and Weisberg, J. B. 2000. The GATF Practical Guide to Color Management. GATFPress, Second Edition.

ANSI IT8.7/2-1993 (ISO 12641), Graphic Technology - Color Reflection Target for Input Scanner Calibration (see http://www.npes.org/standards/descript.htm for ordering information).

Archer, H. B. 1954 . Reproduction of Gray with Halftones. TAGA Proc., 6, 180-193.

Bak, C. Oct. 1997. Color: From Art to Science. In-Plant Graphics 33.

Bala, R. Nov. 6-9, 2001. What is the Chrominance of "Gray"?. Proceedings of the 9th Color Imaging Conference, Sponsored by IS&T and SID, Scottsdale AZ, , p 102.

Brues, S. 2000. Postscriptum on Color Management, GretagMacbeth, Second Edition.

Carli, D. Oct. 1993. Screening: Making Order Out of Chaos. High Volume Printing, 11, No. 5, 24.

CGATS TR001, Graphic Technology- Color Characterization for Type 1 printing.

CIE Proceedings 1931, 1932. Cambridge University Press, Cambridge.

CIE, Recommendations on Uniform Color Spaces, Color-Difference Equations, Psychometric Color Terms, Supplement No. 2 of CIE Publ. No. 15 (E-1.3.1) 1971, 1978. Bureau Ventral de la CIE, Paris

Eastman Kodak, 1995. Q-60INSTR.

Fischer, G. 1989. A Screenless Electronic Imaging Process Using Frequency Modulation. TAGA Proceedings, 195

Fleming, P. D., Cawthorne, J. E. Mehta, F. Halwawala, S. and Joyce, M. K. 2003. Interpretation of Dot Area and Dot Shape based on Image Analysis. Journal of Imaging Science and Technology, 47, 394.

Fleming, P. D. and . Sharma, A. August, 2002. Color Management and ICC Profiles: Can't Live Without It so Learn to Live with It. Gravure, 56.

Green, P. 1999a. Understanding Digital Color, 2nd Edition, GATFPress, Chapter 1.

Green, P. 1999b. Understanding Digital Color, 2nd Edition, GATFPress, Chapter 2, p41.

Green, P. 1999c. Understanding Digital Color, 2nd Edition, GATFPress, Chapter 4, 104-107.

Green, P. 1999d. Understanding Digital Color, 2nd Edition, GATFPress, Chapter 6, pp150-155.

Green, P. 1999e. Understanding Digital Color, 2nd Edition, GATFPress, Chapter 7.

Groff, P.J. and Kanonik, Frank V. 1990a Test Images for Printing. GATFPress 13.

Groff, P.J. and Kanonik, Frank V. 1990b Test Images for Printing. GATFPress 71.

Gustavson, S. May/June 1997. Color Gamut of Halftone Reproduction. J. Imag. Sci. & Tech., 41 (3) 283.

Haneishi, H., Shiobara, T. and Miyake, Y. 1995. Color correction for colorimetric color reproduction in an electronic endoscope. Optics Comm. 114, 57.

ICC home page, http://www.color.org.

ICC, Specification ICC.1:2001-12, File Formats for Color Profiles (version 4.0.0), downloadable from http://www.color.org.

Imai, F. H., Tsumura, N. Haneishi, H. and Miyake, Y. Mar./Apr. 1997. Prediction of Color Reproduction for Skin Color Under Different Illuminants Based on Color Appearance Models. J. Imag. Sci. Tech. 41 (2) 166.

Ker, J., Hsu, CY Kuo and Liu, B 1997. A Fuzzy CMAC Model for Color Reproduction. Fuzzy Sets and Systems, 91, 53.

Khandekar, A. D. April 2001. Color Management with Three process Colors: Application to a Color Laser Printer and a Flexographic Press. MS Thesis, Western Michigan University.

Khandekar, A. D., Fleming, P. D. Pekarovicova, A, and Joyce, M. K. CMY Color Management; Application to a Color Laser Printer and a Flexographic Press. In Preparation.

Lee, H.K., Joyce, M.K. Fleming, P.D. and, Cameron, J. May 2002. Production of a Single Coated Glossy Inkjet Paper Using Conventional Coating and Calendering Methods. Proceedings of the TAPPI Coating Conference.

Martens, J. Oct. 1997. Color Management Using CIELab, Flexo p60.

McDowell, D. April 2002. Color Management: What's New with the ICC?, Gravure 50-54.

Molla, R. K. 1988. Electronic Color Separation, RK Printing and Publishing Co., West Virginia 34.

Murray, A. 1936. Monochrome Reproduction in Photo-Engraving. J. Franklin Inst. 221, 721-744.

Nothman, G. A. 1989a. Nonimpact Printing, GATFPress,, Chapter 7, 78-79.

Nothman, G. A. 1989b. Nonimpact Printing, GATFPress,, Chapter 7, 80-83.

Pfiffner, P. and Fraser, B. 1994. How Desktop Publishing Works Ziff-Davis Press Chapter 11.

Preucil, F. 1964. Some Additive Color Principles and the Control of Neutral Grays in Process Reproduction. Halftone Printing, W. H. Banks ed. Pergamon Press, Oxford 75-84.

Rich, D. C. Oct. 1997. Today's Color Management Systems: The Application of Advanced Technology to the Science of Color, American Inkmaker 60.

Rong, X. December 2003. Color Management and Input Device Profiling. MS Thesis, Western Michigan University.

Rong, X. April 14-17 2002. Gray Balance and its Effect on the Quality of Input Profiles. TAGA Student Paper, TAGA Annual Technical Conference in Asheville, North Carolina.

Samworth, M. Mar., Apr., May, 1998. Toward True Color Management, Part 1-3, Flexo, 74, 64, 57.

Schildgen, T. E. 1998a. Pocket Guide to Color with digital applications. Delmar chapter 3.

Schildgen, T. E. 1998b. Pocket Guide to Color with digital applications. Delmar chapter 4.

Sharma, A. 2003a. Understanding Color Management, Delmar Learning.

Sharma, A. and Fleming, P. D. January 13, 2003b. Measuring the Quality of ICC Profiles and Color-Management Software. Seybold Report, Vol. 2, No. 19, 3-8.

Sharma, A. and Fleming, P. D. January 1, 2003c. Measuring the accuracy of ICC profiles and color management software. WMU Profiling Review 3.0. This can be obtained by sending an email to abhay.sharma@wmich.edu with "Subscribe WMU Profiling Review" in the subject line.

Sharma, A. and Fleming, P. D. April 11-14, 2002a. Evaluating the Quality of Commercial ICC Color Management Software. Proceedings of the TAGA Annual Technical Conference, North Carolina.

Sharma, A., Gouch, M. P. and Rughani, D. N. 2002b. Generation of an ICC Profile from a proprietary style file. J. Imag. Sci. Tech. 46:26.

Sharma, A. July/August, 2002c. Photoshop 7.0: Revolutionary or Evolutionary? Photo Techniques.

Stanton, A. P. and Warner, R. D. 1994. Color Reproduction Characteristics of Stochastically Screened Images. TAGA Proceedings 65.

SWOP. 2001. SWOP for the New Millennium, Specifications for Web Offset Publications, Published by SWOP Incorporated, NY, 9th edition.

Tolliver, H. Oct. 1997. Quantifying Color. American Inkmaker 16.

Widman, J. Ed. summer, 1998. Flat-Panel Power. Publish Extra.

Williamson, K. C. Nov/Dec 1997. A Soft Proofing Study. GATF World 23.

Zhang, X. and Wandell, B.A. 1997. A Spatial Extension of CIELab for Digital Color-Image Reproduction. JSID, 5/1, 61.